Pergamon

Journal of Structural Geology, Vol. 16, No. 4, pp. 603 to 612, 1994

0191-8141/94 $6.00+0.00

0191-8141(93)E0005-6

Fault scaling laws and the temporal evolution of fault systems

STEVEN F. WOJTAL

Department of Geology, Oberlin College, Oberlin, OH 44074, U.S.A.

(*Received* 3 *February* 1993; *accepted in revised form* 28 *October* 1993)

Abstract—Through an analysis of the temporal evolution of duplex fault systems, this contribution shows that it is unlikely that all faults in a deformed area will conform to a single frequency–size scaling relationship. The development of a duplex leads to different size–frequency relationships for the faults that compose the duplex and those confined to individual horses. The faults that compose the duplex define segments with relatively steep slopes on a log N (number of faults, i.e. frequency) vs log D (displacement magnitude, i.e. size) plot; faults within individual horses define segments with relatively shallow slopes on a log N vs log D plot. The distinction between these two types of faults in a duplex is akin to the distinction between large active faults, which cut the entire seismogenic layer, and small active faults, which do not extend across the seismogenic layer. If, as is often the case, the faults that compose a duplex do not extend across the seismogenic layer, the stepped nature of the resulting log N vs log D plot may make it particularly difficult to assess the contribution of these 'small' faults to regional deformation. Since duplex geometries result in part from anisotropies present in deforming rocks, the anisotropy present in nearly all crustal rocks will affect the size–frequency relationship observed for systems of faults. Different parts of a deforming rock mass are likely to have different initial anisotropies. Combining data on fault systems from markedly different portions of a deforming region may, then, obscure the unique characteristics of the size–frequency relationship in either area and may lead to inaccurate assessments of the relative contributions of 'small' and 'large' faults to regional fault-accommodated strains.

INTRODUCTION

RECENT investigations of fault systems emphasize the scale invariance of the fundamental characteristics of faults and suggest that simple relationships exist between the lengths of individual faults or the widths of individual fault zones and the magnitudes of slip on them (Elliott 1976, Watterson 1986, Hull 1988, Walsh & Watterson 1988, Marrett & Allmendinger 1990, 1992, Scholz & Cowie 1990). One potentially far reaching result of these studies of fault populations is the proposal that faults follow a power-law scaling for their size–frequency distributions (Scholz & Cowie, 1990, Marrett & Allmendinger 1991, 1992, Cowie & Scholz 1992a, b). The attraction and utility of demonstrating a single scaling law for all faults in a deformed region is apparent, particularly for geologists interested in measuring strain. Data on faults gathered within a limited range of lengths could then determine accurately fault characteristics, fault spacing and the relative contributions of faults to total strain across several orders of magnitude of lengths. Moreover, such scaling laws might provide the key to relating the measurable characteristics of natural fault populations in deformed regions to the observed frequencies of earthquakes in seismically active areas (Scholz & Cowie 1990, Hanks 1992).

This contribution considers the temporal evolution of hypothetical and natural fault systems, focusing on *displacement populations* (Marrett & Allmendinger 1990) for faults in fold–thrust belts, in order to examine how fault system evolution might affect the power-law scaling and thereby change how fault systems accommodate strains. This examination identifies several reasons why fault displacement populations from individual regions may depart from power-law size–frequency distributions. Some departures can be anticipated by noting that different faults or fault segments accrue slip in different ways or that individual faults accrue slip in different ways at different times. For example, some fault zones or sections of fault zones thicken and others thin as displacement accrues across them (Means 1984, Hull 1988); individual fault zones or sections of a fault zone may thicken at one time and thin at another (Wojtal & Mitra 1988). Changes in the thickness of active fault zone would change the rates of nucleation and growth of small faults associated with the major fault. Other departures result from interactions between faults or reflect the anisotropy present in nearly all crustal rocks. Body deformation constitutes a measurable fraction of the total deformation even where faulting is the dominant deformation mechanism (Jackson & McKenzie 1988, Ekstrom & England 1989), and continuous deformation affects how slip is partitioned among faults. Because diffusion contributes to many continuous deformation processes and because diffusion depends explicitly upon a length scale and usually varies with spatial orientation, the partitioning of displacement among small and large faults with different orientations will differ. These departures from self-similarity reduce the reliability of assessments of the total deformation from fault data collected within a limited range of observation scales. Finally, since these parameters will differ in different tectonic environments, this analysis underscores the dangers of compiling fault data from

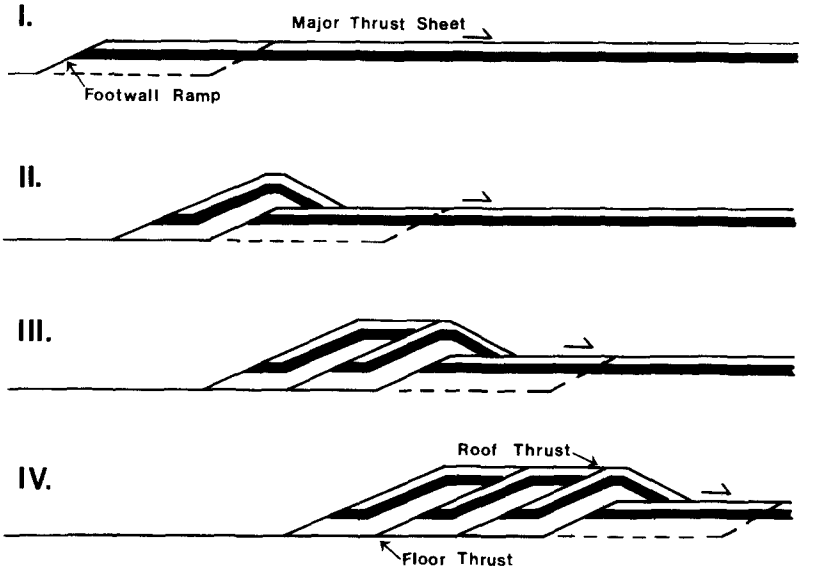

Fig. 1. Model for duplex development redrawn from Boyer & Elliott (1982).

different portions of a single deformed region or from numerous deformed regions in an attempt to define universal scaling laws.

VIEWS OF FAULT POPULATIONS

Figure 1, the archetypal view of duplex development from Boyer & Elliott (1982), is widely accepted and reproduced because it summarizes concisely and accurately the observations of numerous examinations of the geometry of natural thrust systems. Acceptance of this model by workers examining faults in extensional (e.g. Gibbs 1984) or transcurrent regimes (Woodcock & Fischer 1988, Swanson 1990) indicates that the duplex model identified a characteristic feature of fault systems. The duplex geometry is, to some degree, scale-independent; geologists have identified crustal-scale duplexes, map-scale duplexes, outcrop-scale duplexes and thin-section-scale duplexes. The fundamental geometry of the duplex model depends, however, on the scale of the anisotropy of the deforming layers, i.e. what are the spacings between glide horizons (flats) or between imbricates (ramps). In order to apply the duplex model of fault development to a particular area, one must know intimately the geometry, kinematics, and mechanics of faults in the area, i.e. where to place the roof and floor thrusts, what is the spacing of the imbricates, or how displacement is partitioned among the several imbricates. The power of the duplex model lay in relating observations of faults to systematic patterns and in its emphasis on the temporal evolution of the geometry of fault systems.

Figure 2 presents several displacement populations for faults, a view of fault systems that is rapidly becoming as exemplary and widely accepted as the duplex model. Plots like those in Fig. 2 are widely reproduced and accepted because they too describe concisely and accurately fundamental characteristics of fault systems, in this case an inferred power-law scaling relationship between the magnitude of fault slip and the frequency of fault occurrence. A power-law scaling relationship, in this case between the numbers of faults and fault displacement, suggests self-similarity (Schroeder 1990, pp. 103–119). Kakimi (1980), Villemin & Sunwoo (1987), Scholz & Cowie (1990), Walsh *et al.* (1991), Marrett &

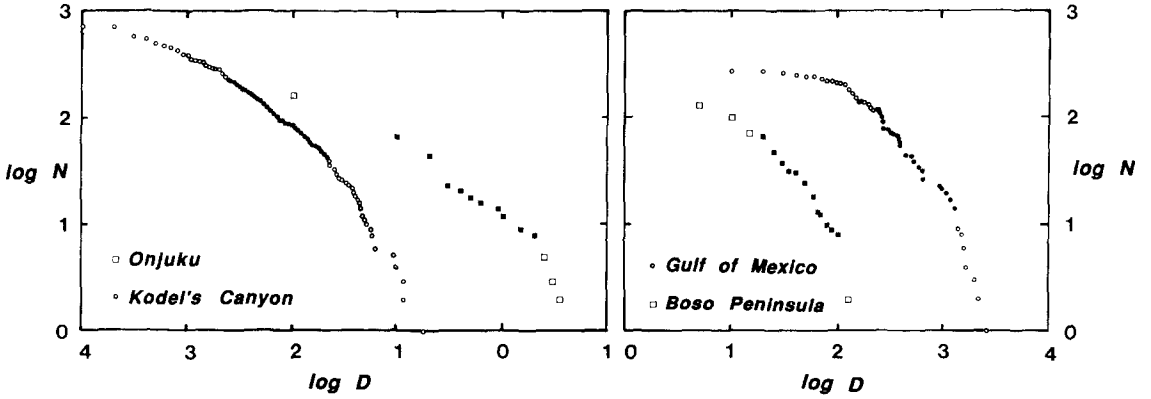

Fig. 2. Displacement populations for faults from Marrett & Allmendinger (1992). Boso data originally from Minor Faults Research Group (1973). Onjuku data from Kakimi (1980) and Kodel's Canyon data from Jamison (1989). Each plot derived from an ordered list of all faults observed in the area, with logarithm of a fault's ordinal number plotted against the logarithm of its displacement. Filled symbols denote those portions of fault populations that Marrett & Allmendinger (1992) inferred to conform to power-law size–frequency relationships. D = displacement in meters.

Allmendinger (1992) and others have inferred power-law size–frequency relationships for faults in specific areas, and have used the inferred self-similar nature of faulting to quantify the regional deformation. As is the case with the duplex model, one must know intimately faults in a given area in order to determine the specific scaling law that pertains to faults in that area. Since very few fault populations are sufficiently well known to fix the scaling laws, data gathered in a few carefully studied locations (Minor Faults Research Group 1973, Kakimi 1980, Jamison 1989, Childs *et al.* 1990, Walsh *et al.* 1991, Marrett & Allmendinger 1992) are cited repeatedly. If faults follow predictable scaling laws, these carefully studied examples provide insight to the fundamental processes that control faulting everywhere.

Views of fault systems derived from a characterization like the duplex model, which emphasizes the temporal development of faults, and views of fault systems derived from a characterization like a displacement population, which emphasizes the collective character of fault populations at a particular instant, have remained mutually exclusive to date. The two views must reconcile with each other before one can reliably use fault system characteristics collected over a limited range of length scales to estimate finite strain magnitude over all length scales. One step toward reconciling these two points of view is to examine the instantaneous properties of seismically-active fault systems. Aviles *et al.* (1987) and Okubo & Aki (1987) concluded that the active San Andreas fault system is not geometrically self-similar over all length scales, and Hirata (1989) drew similar conclusions about active fault systems in Japan. First, fault scaling laws varied with geographic position for both fault systems. In addition, changes in the fault-scaling law at individual locations apparently coincide with a change from small, unbounded faults, which do not extend across the seismogenic layer, to large, bounded faults, whose widths equal the thickness of the seismogenic layer (cf. Scholz & Cowie 1990, Pacheco *et al.* 1992). In the San Andreas fault system, other size-dependent changes in fault geometric character occur at lengths other than the thickness of the seismogenic layer (1–2 km in Aviles *et al.* 1987, 500 m in Okubo & Aki 1987). The cause of the latter change is not clearly defined, although it may relate to interactions between members of fault systems. Neither is it clear how the distribution of slip increments among one set of active faults evolves into the distribution of net slips among a comparable set of faults in deformed rocks (cf. Walsh *et al.* 1991). Nevertheless, some have inferred that a single scaling law holds over many orders of magnitude of size, i.e. that faults are self-similar, and that data collected over some range of length scales can constrain inferences on the magnitudes of strains outside the range of observations (cf. Scholz & Cowie 1990, Marrett & Allmendinger 1991, 1992).

Linear plots of the logarithms of the numbers of faults (log N) vs logarithms of their displacement (log D) constitute one basis of the inference of self-similarity for faults (Scholz & Cowie 1990). While most workers emphasize the linear nature of log N vs log D plots and infer uniform fault scaling laws over several orders of magnitude, displacement populations typically define *faceted plots* (Fig. 2). Marrett & Allmendinger (1992) argue that faceted plots result from two kinds of sampling bias: (1) at the smallest displacement values, practical difficulties in counting every fault cause departures from the linear log N vs log D; and (2) at the largest displacement values, combinations of fault data collected in two or more adjacent traverses, or anomalous counts of faults in some displacement classes resulting from limits imposed by the scale of the map or section from which the data were collected, cause departures from the linear log N vs log D plot. Examining the effects of the temporal evolution of fault systems on displacement populations, however, shows that some departures from linearity are not artifacts of sampling; they can be anticipated by examining the evolution of fault systems. If factors other than sampling bias cause distinct changes in the slope of a log N vs log D plot, the population is multifractal or pseudofractal (Whalley & Orford 1989). I suggest here that many fault populations are multifractal, and examine some causes for departure from fractal or self-similar behavior. Often, one knows about these factors prior to constructing log N vs log D plots, for one must know a fault population intimately in order to construct the log–log plot. There are, however, situations where the plot itself can provide some insight to the fault system.

EVOLUTION OF FAULT SYSTEMS

Effects on large faults of partitioning slip onto selected faults

If a fault system in an area were truly self-similar, then the exponent in its power-law relationship would not change with time (Fig. 3). Does such an inference

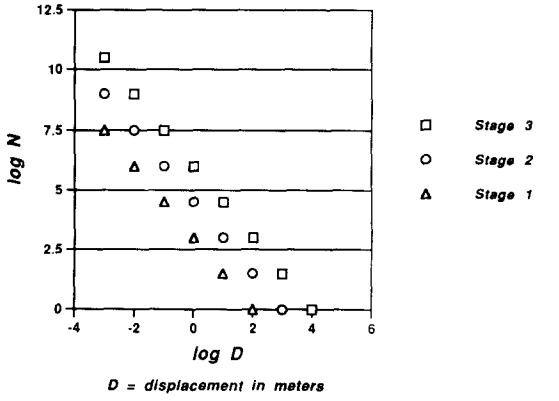

Fig. 3. Plot showing three stages in the evolution of a hypothetical fault population that grows with a constant size–frequency relationship, $N \propto D^{-C}$. The value of C, which defines the slope of the log N vs log D curve, was chosen arbitrarily as 1.5. This value for the slope is within the range of observed values (Scholz & Cowie 1990, Marrett & Allmendinger 1992). The increase in the total number of faults as deformation proceeds indicates that nucleation of new faults accompanied deformation.

pertain to fold–thrust belt fault systems that conform with the geometries and temporal evolution commonly observed in those belts? To estimate how successive log N vs log D plots in a area would look, I constructed hypothetical log N vs log D plots for different stages in the evolution of simple thrust system geometries. I *assume* self-similarity for faults within each horse in the thrust system. Thus, the displacement magnitude of the individual bounding faults predicts directly the number of faults with smaller displacements. The assumption of self similarity scaled to the displacement of major thrusts derives from two observations on the development of faults in thrust belts. First, the rocks adjacent to major thrust faults are often cut by arrays of minor faults (Harris & Milici 1977, Platt & Leggett 1986, Wojtal 1986); the thickness of the intensely faulted rock adjacent to a major fault may scale, at least during the first slip increments, with the displacement magnitude on the major fault (Robertson 1982, 1983, Hull 1988, Evans 1990, Holl & Anastasio 1992). Second, as displacement on a major thrust fault increases, a larger mass of hangingwall with one original shape must conform to a footwall template with a different shape. If the deformation that allows the hangingwall to conform to its new footwall template occurs by faulting, the number of small faults in the region must increase (new faults must nucleate). I *assume* initially that these faults also scale with the magnitude of the major thrust faults.

Major faults usually define imbricate or duplex fault systems. In the standard duplex of Boyer & Elliott (1982), the partitioning of slip onto a specific subset of faults produces a steep slope for the segment of a log N vs log D plot corresponding to the slip magnitudes of the imbricates (Fig. 4a). In an ideal or flat-roofed duplex, the slope of this segment of the log N vs log D plot is essentially vertical. Most real duplexes have unequal slip on the imbricates (Mitra 1986, Tanner 1992a, b), yielding steep but not vertical slopes for segments of the log N vs log D plots (Fig. 4b).

The standard duplex model presumes that imbrication occurs only in the footwall and that each footwall imbricate forms as a unit. Duplexes may form in other ways provided that they conform with constraints on the growth of individual faults. Some recent analyses of the formation of faults in fold–thrust belts suggest that detachment surfaces grow to significant size before they accrue significant slip (Fischer & Woodward 1992, Armstrong & Bartley 1993). If, as suggested by Eisenstadt & De Paor (1987), imbricates form independently within a layer between two detachments and propagate toward those upper and lower detachment horizons, imbricates could form simultaneously. Such a sequence also leads to steepened slopes on log N vs log D plots for the larger offset faults, although there could be distinct large displacement faults corresponding to the detachments and the imbricates. Boyer (1992) reviewed several other kinematic alternatives to the footwall imbrication mechanism. Combining the assumption that small faults within fault-bounded horses scale relative to the bounding faults with Boyer's models for synchronous or alternating movement on major thrusts also yields log N vs log D plots with steep slopes in the displacement range corresponding to the slip magnitudes of the imbricates (Fig. 5). Finally, the individual major faults within imbricate systems as defined by Boyer & Elliott (1982) often have comparable slip magnitudes, again yielding log N vs log D plots with steep slopes in the displacement range corresponding to the slip magnitudes of the imbricates (Fig. 6).

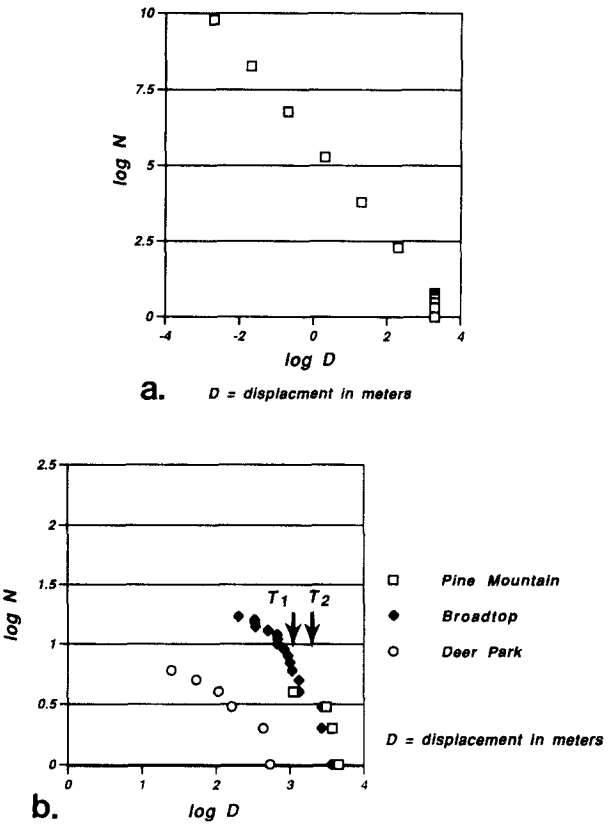

Fig. 4. (a) A log N vs log D plot for a hypothetical duplex, drawn following the model of Boyer & Elliott (1982), composed of six horses. As outlined in the text, the number of faults *within* each horse was scaled to the displacement magnitude of the horse's bounding fault by a single power-law size–frequency relationship. Note the steep slope at the displacement magnitude corresponding to the slip on the horse-bounding faults. (b) Log N vs log D plots of the largest faults in three duplexes from Mitra (1986). Pine Mountain refers to the southern Appalachian thrust fault system depicted in fig. 14 of Mitra (1986). Broadtop refers to the inferred blind thrust system in Siluro-Devonian strata beneath the central Appalachian Broadtop synclinorium depicted in fig. 18 of Mitra (1986). Deer Park refers to the blind duplex in Ordovician strata beneath the central Appalachian Deer Park anticline depicted in fig. 27 of Mitra (1986). In each case, the major faults define relatively steep lines corresponding to the typical slip magnitude on imbricates. Arrows labeled T_1 and T_2 denote the log of the stratigraphic thickness between floor and roof thrusts for the Deer Park and Broadtop and the Pine Mountain duplexes, respectively. The steep slopes on these plots roughly conform with the position of log T_i for each duplex.

The distinction between two classes of faults in any duplex system, those that constitute the duplex itself and those that accommodate the deformation within fault-bounded horses, mirrors to some degree the distinction between 'small' and 'large' faults in seismically active systems (Scholz & Cowie 1990). In an individual duplex, these different segments of the total population of faults should, like small and large active faults (cf. Pacheco *et*

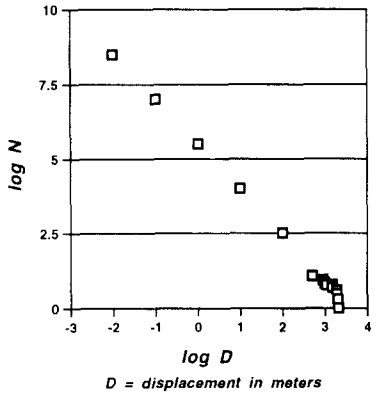

Fig. 5. A log N vs log D plot for the synchronous movement model of imbrication described by Boyer (1992). The number of faults *within* each horse in a hypothetical section with synchronous movement on four major thrusts (fig. 8 from Boyer 1992) was scaled to the displacement magnitude of the horse's bounding fault with a single power-law size–frequency relationship. Once again, there is a steep slope at the displacement magnitude corresponding to the slip on the horse-bounding faults.

al. 1992), exhibit different slopes on a log N vs log D plot. The change in the slope of the log N vs log D plot, which occurs at a displacement value $D^* \approx T$, the net thickness of imbricated strata (Fig. 4b), indicates that the fault systems in duplexes are multifractal, or not self similar across all length scales. The duplex equivalents of 'large' faults, whose displacements are greater then D^*, exhibit relatively steep slopes on log N vs log D plots. The duplex equivalents of 'small' faults, whose displacements are less then D^*, apparently keep relatively shallow slopes on log N vs log D plots.

Effects on small faults of partitioning slip onto selected faults

It is, of course, axiomatic that fold–thrust belt shortening occurs by localizing deformation in major thrust fault zones, leaving relatively undeformed thrust sheets. To consider further the effects of this localization of deformation on the log N vs log D plots in an area, I

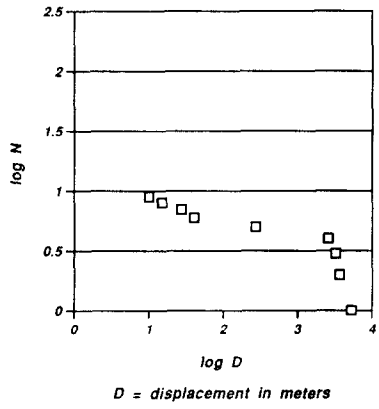

Fig. 6. A log N vs log D plot of the major faults from the eastern half of the Sawtooth Range imbricate system is depicted in fig. 19 of Mitra (1986). These faults define a relatively steep line, like the case of duplex systems (see Fig. 4).

briefly recast data on fault zone development derived from some southern Appalachian thrust zones. The data on fault zones come from detailed examinations of the hangingwalls of the Cumberland Plateau and Copper Creek thrusts (Harris & Milici 1977, Wojtal 1986). The Cumberland Plateau thrust, which crops out at the west side of the southern Appalachian foreland fold–thrust belt, has a displacement magnitude on the order of 1–3 km. The Copper Creek thrust, which crops out near the center of the southern Appalachian foreland fold–thrust belt, has a displacement between 16 and 20 km. Arrays of minor faults adjacent to these major thrusts share many characteristics with other well-known fault populations.

The N vs log D plot for mesoscopic contraction faults adjacent to the Cumberland Plateau thrust (Fig. 7a) has a relatively linear middle segment with a slope of -1.17. Faults with displacements less than 50 cm plot below the line whose slope is -1.17. Likewise, faults with displacement on the order of 5 m plot below the line whose slope is -1.17. The low slope for small displacement faults may be an artifact of sampling. The steep slope for large displacement faults is not likely to result from errors in measuring fault displacements (mapped on 1:25 photographs), from effects related to the size of the sampling area (the fault data were collected from a section whose total area is over 13,000 m^2), or from effects of a small size for the sampling window (which pertains more to measurements of fault length not fault displacement), factors to which steep slopes have been attributed (Marrett & Allmendinger 1992). This steep slope derives, I believe, from preferential partitioning of slip onto a limited number of faults within the population. The change for 'small' to 'large' faults in this system occurs at displacement $D^* \approx 5$–10 m (Fig. 7a).

The N vs log D plot for mesoscopic contraction faults adjacent to the Copper Creek thrust (Fig. 7b) shows similar characteristics. The plot has a nearly linear segment with a slope of -0.725 for faults with displacements between 1 and 10 m. Faults with displacements less than 1 m plot below that line, and faults with displacements greater than 10 m define a separate relatively steep segment below that line. The departure from linearity at small displacements is most assuredly due to undercounting faults with small displacements. The steep segment defined by faults with large displacement might be a sampling artifact, but it probably results from preferential partitioning of slip onto some faults. I infer that this change in slope signals a change from 'small' to 'large' faults, occurring in this system at displacement $D^* \approx$ 10–40 m (Fig. 7b). The relatively shallow slope, -0.725, of the middle linear segment of this log N vs log D plot, derived from faults with offsets of the order of 1 m and lengths of several meters, suggests that the fault population in this thrust sheet differs significantly from that in the Cumberland Plateau thrust sheet.

A shallow slope on a log N vs log D plot implies that small faults make a relatively less significant contribution to the overall strain; a steep slope implies that small faults are significant contributors to total defor-

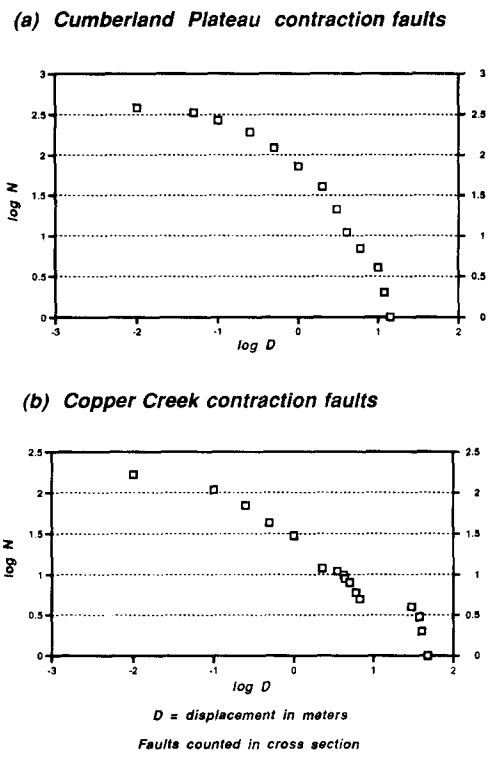

Fig. 7. (a) A log N vs log D plot of small contraction faults from the hangingwall of the Cumberland Plateau thrust of the southern Appalachians (Wojtal 1986). The data were collected on a profile constructed using 1:50 photographs and a 1:1200 plane table map; total area of the section is 13,732 m^2. The raw number of faults counted is 279, but the numbers of faults in different displacement classes at different distances from the thrust were adjusted to account for an equal width of counting area along a traverse normal to the thrust surface. This adjusted number of faults is 381. Taking $N = AD^{-C}$, $C = 1.17$ for the central linear segment of the plot (this value comes from a linear fit to the central part of the log–log plot with $\log A = 1.822$ and $r = 0.979$). Considering only the larger faults, $N = AD^{-C}$, with $C = 4.11$ for the three largest faults on the plot (this value also comes from a linear fit of that part of the log–log plot with $\log A = 4.702$ and $r = 0.999$). The two linear log–log curves intersect at a value of $\log D = 0.979$ or $D = 9.6$ m. (b) A log N vs log D plot for small contraction faults from the hangingwall of the Copper Creek thrust of the southern Appalachians (Wojtal 1986). These data were also collected on a profile constructed using 1:50 photographs and a 1:1200 plane table map; the total area of the section is 6612 m^2. The raw number of faults is 135, but the numbers of faults in different displacement classes at different distances from the thrust were adjusted to account for an equal width of counting area along a traverse normal to the thrust surface. This adjusted number of faults is 167. Taking $N = AD^{-C}$, $C = 0.725$ for the central linear segment of the plot (this value comes from a linear fit to the central part of the log–log plot with $\log A = 1.419$ and $r = 0.991$). Considering only the larger faults, $N = AD^{-C}$, with $C = 4.65$ for the three largest faults on the plot (this value also comes from a linear fit of that part of the log–log plot with $\log A = 7.497$ and r = 0.987). The two linear log–log curves intersect at a value of $\log D = 1.625$ or $D = 42$ m.

mation (Marrett & Allmendinger 1992). Comparing the slope for 'small' faults on the log N vs log D plot from the Cumberland Plateau fault zone (total slip = 1–3 km) with that for 'small' faults from the Copper Creek fault zone (total slip = 16–20 km) indicates that small faults are more important in the former than in the latter. Two factors suggest that this is the correct inference to draw from these faults zones. First, by modeling faults as discontinuities with infinitesimal Burger's vectors, Wojtal & Mitra (1986) argued that faulted rocks may mechanically harden. Second, the episodic shortening and elongation of thrust zones (Woodward *et al.* 1988) often leads to geometrical hardening due to cross-cutting faults. Either factor could lead to the preferential partitioning of slip onto a limited number of faults within the region during later deformation increments. The increase in displacement on that limited number of faults could occur without the nucleation and growth of new small displacement faults, thereby leading to a shallower slope on a log N vs log D plot (cf. Kakimi 1980).

These two factors could also cause the fault-related deformation to be partitioned preferentially into undeformed rock at the margin of the major fault zone, i.e. cause the major fault zone to thicken. Thickening of the fault zone could lead to the nucleation of new faults, tending to preserve the original log N vs log D slope for small faults. A correlation exists between the thickness of deformed zones near major thrusts and the displacement on the thrusts (Hull 1988, Evans 1990, Holl & Anastasio 1992). The correlation breaks down at larger displacement values for major thrust faults, however, primarily because fault zone material properties change as fault zone structure evolves (Means 1984, Hull 1988). In particular, arrays of minor faults form an interconnected network for percolating fluids (Rye & Bradbury 1988, Wiltschko & Budai 1988, Grant *et al.* 1990, Roberts 1990, Bruhn 1992). The presence of pore fluids may lead to the concomitant development of distinctive fault rocks and dramatic changes in fault zone mechanical properties (Mitra 1984, Wojtal & Mitra 1986, Wojtal 1992). Thus while fault zones may become thicker during initial slip increments, eventually the most active portion of a fault zone is a narrow layer dominated by banded cataclasites, pervasively cleaved rocks, or some combination of the two (Wojtal & Mitra 1988, Woodward *et al.* 1988). This process is apparently accompanied by changes in mesoscopic fault populations (Wojtal 1986), where slip is apparently partitioned preferentially onto a subset of all minor faults. If small faults are less important, slopes on log N vs log D plots become shallower (Kakimi 1980) (Fig. 8). Figures 7(a) & (b) may then represent different stages in a temporal evolution, with Fig. 7(a) depicting in a crude way how

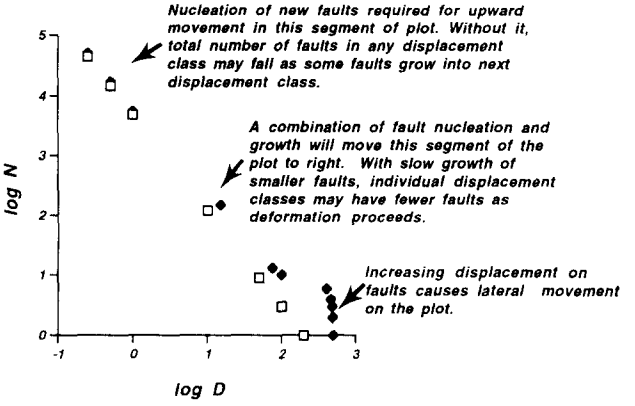

Fig. 8. A log N vs log D plot showing one possible way a fault population that initially conforms to a power-law size–frequency relationship, denoted by the open symbols, might change as slip is partitioned on a set of faults to form a duplex. Filled symbols show the population after the formation of the duplex. This process might occur at several scales, generating faceted plots like those seen in Fig. 2.

the fault population in Fig. 7(b) might have appeared at an earlier time. Temporal changes in the manner in which slip is partitioned among faults can also, then, reduce the importance of 'small' faults and enhance the tendency for faceted log N vs log D plots.

DISCUSSION

Interactions between faults occur throughout all real deformations, often leading to a duplex geometry. As a collection of faults evolves into the linked duplex system, the collective character of the fault system changes in two interrelated ways. The faults that become the ramps and flats of the duplex accrue slip until they have relatively large, approximately equal displacements. Once they attain this displacement magnitude, further increases in displacement occur in conjunction with slip increases on interconnected faults. On a log N vs log D plot, the ramp and flat faults define a segment with a relatively steep slope. The ramp and flat faults are akin to 'large' active faults (Scholz & Cowie 1990, Pacheco *et al.* 1992), i.e. their growth is 'bounded'. Ramp and flat faults exhibit population dynamics different from those they exhibited earlier in their history, and these population characteristics are different from other faults in these rocks. The faults that accommodate deformation within fault-bounded blocks are akin to 'small' active faults (Scholz & Cowie 1990, Pacheco *et al.* 1992), i.e. their growth remains 'unbounded'. It is conceivable that these small faults could exhibit similar population dynamics throughout deformation. It is possible, however, that the population dynamics of the small faults within a duplex also change as deformation proceeds, that they make proportionally smaller contributions to the total strain during later increments (Kakimi 1980, Wojtal 1986), and they therefore define shallower slopes on log N vs log D plots later in the deformation. In either case, the formation of a duplex leads to a faceted log N vs log D plot (Fig. 8). The faceted nature of the plot indicates the faults in duplexes are multifractal.

Implications for estimating fault-accommodated strains

The distances between flats in regional duplexes, which reflect large-scale tectono-stratigraphic patterns, will control the position of the most easily noted break in slope on a log N vs log D plot (Fig. 4b), that separating the steep segment corresponding to the regional imbricates and glide horizons from shallower segment for smaller faults. It is not uncommon to find smaller duplexes along the major faults of a larger duplex (Swanson 1990, Tanner 1992a). The recognition of nested duplexes is in itself an acknowledgement of a measure of scale independence to a deformation. The behavior of all smaller faults in nested duplexes is not the same, however. Displacement is partitioned preferentially to faults with a limited range of linear dimensions and slip magnitudes (i.e. those that compose the duplexes) and not to faults with different (i.e. intermediate) linear dimensions and slip magnitudes. This partitioning should lead to log N vs log D plots with numerous steps, where steeper segments of the log N vs log D plot correspond to ramp and flat faults within duplexes and shallower segments correspond to the faults that accommodate deformation of fault-bounded horses.

Even if sampling of faults in a deformed area were perfect, details of the stepped nature of the log N vs log D plot could be difficult to recognize. The distance between flats in smaller duplexes reflects the thickness of relatively competent strata, and bed thicknesses in many stratigraphic sequences are log-normally distributed (Pettijohn 1957, p. 160). Normally, sampling from a sizable area is necessary in order to obtain sufficiently large numbers of faults for statistical treatments. In any sizable deformed region, the total number of faults N_i with displacement D_i is likely to include ramp or flat faults from duplexes of one particular size and faults that accommodate intra-horse deformation in larger duplexes. This mixing of different types of faults could obscure the population dynamics of either of these fault types and could lead to erroneous conclusions on the dynamics of or strain accommodated by either fault type. Given the manner in which many workers sample fault populations, where relatively small numbers of faults counted in detailed studies of small areas, profiles, or lines transects are somehow adjusted to estimate the fault distribution in a larger area, it is perhaps equally likely that the calculated or estimated log N vs log D plot will preserve or accentuate steps due to duplexes of one size in the sample area that do not persist throughout the entire deformed area. This too will decrease the accuracy of inferences on the dynamics of or strain accommodated by 'small' faults.

The average slope of the log N vs log D plot measures the average contribution of faults to the regional strain (Marrett & Allmendinger 1992). In the two data sets presented here, the slopes vary from values close to -1 for smaller faults and to values on the order of -4 for large faults (Fig. 7). The relative magnitudes of the slopes give the relative importance to the total deformation of faults within a range of displacement classes. It is difficult to decide, however, whether a slope of -1, a slope of -4, or an average value best characterizes the overall contribution of these small faults to the total deformation in these rocks. An average slope may not accurately represent either component of the actual fault population, and it cannot, in any case, indicate how strain is partitioned within the deformed rock. Independent assessments of strain intensity, such as measurements of displacement gradients or documentation or rotation of fold axes toward parallelism with an inferred transport direction (Wojtal 1986), indicate that strains are relatively lower in the Cumberland Plateau sheet than in the Copper Creek sheet. The inference that small faults contribute less to the total deformation in the Copper Creek sheet (Fig. 7b) than in the Cumberland Plateau sheet (Fig. 7a) must not be misinterpreted to indicate the relative magnitude of fault-accommodated strain is lower in the Copper Creek sheet.

Implications for the mechanics of faults and fault systems

All faults from the Cumberland Plateau and Copper Creek thrust sheets in Fig. 7 are 'small' faults in the regional deformation; none of them define the structural architecture of the individual major thrust sheets or of the orogenic belt. Most faults from the Cumberland Plateau sheet would not appear on 1:10,000 scale maps, and most faults from the Copper Creek sheet are not mapable at a scale of 1:24,000. Nevertheless, these faults fall into separate 'small' and 'large' classes on the log N vs log D plots. The larger of these small faults defining log N vs log D slopes much less than -1, suggesting that they contribute significantly to the total strain. Furthermore, the change in the slope of log N vs log D plot for the 'small' faults in these two cases (at $D \approx 4$–10 m in the Cumberland Plateau sheet and $D \approx 10$–40 m in the Copper Creek sheet) indicates that the importance to small faults can change as deformation proceeds.

In the active San Andreas fault system, the fractal dimension of faults changes with the length scale used for measurement (Aviles *et al.* 1987, Okubo & Aki 1987); faults longer than 0.5–1 km have lower fractal dimensions, i.e. lower sinuosity, than those shorter than 0.5–1 km. Assuming that fault displacement is a constant fraction $\approx$ 5–10% of fault length (Elliott 1976, Watterson 1986, Walsh & Watterson 1988, Cowie & Scholz 1992a), changes fault sinuosity or complexity occur at displacement values of 25–100 m. Curiously, this is approximately the displacement value at which occurs the breaks in the slopes of the log N vs log D plots in Fig. 7. Active faults with slipped areas 100–500 m on a side should generate earthquakes with magnitudes of 2–3 (Sibson 1989). Earthquakes with magnitudes of 2 or less occur at rates lower than expected from examinations of the frequency of earthquakes with magnitudes of 3 to approximately 7 (see for example Pacheco *et al.* 1992). The apparent low frequency of <**M2** earthquakes may result from imperfect detection of the small magnitude events, but it may also relate to a change in fault mechanics due to changes in fault connectivity and sinuosity.

The most significant break in slope on the log N vs log D plots in Fig. 7 may also identify that critical change in fault behavior, where faults that attain lengths of about 500 m or displacements of about 50 m exhibit markedly different mechanics than those with smaller lengths and/or displacements. Whatever the cause, the change relates to a process that varies with the length scale. The examination here suggests that this change in fault mechanics coincides with the formation of mesoscopic duplexes. The formation of duplexes at any scale will alter inexorably the progress and partitioning of later fault-accommodated strain. Once formed, the duplex geometry persists even when displacements on the component faults exceed the length of the horses, and it is able to accommodate significant finite strains (Boyer & Elliott 1982, Mitra 1986). Duplex geometries persist because displacement is partitioned preferentially onto some faults and away from other faults. The sinuosity or complexity and connectivity of faults may be critical in this regard, for interconnected faults provide more continuous networks for fluid infiltration. Fault mechanical behavior changes dramatically due to the physical presence of a fluid phase (cf. Hubbert & Ruby 1959, Sibson 1989), due to changes in the dominant deformation mechanism (Mitra 1984, Wojtal & Mitra 1986), or due to chemical or mineralogical changes in fault rocks (Newman 1993, Newman & Mitra 1993). The partitioning of slip onto some faults may occur because those faults are the smoothest fluid flow paths and have higher pore fluid concentrations.

CONCLUSIONS

Fault systems within an individual orogenic belt are unlikely to exhibit a single power-law size frequency relationship. The natural initial anisotropy of rocks will lead to the formation of duplexes, and duplex formation leads to departures from self-similarity in fault populations. Anisotropy is recognizable as steps or facets in log N vs log D plots for fault populations. Preferential partitioning of slip onto some faults generates a locally steep slope on the log N vs log D plot. A relatively shallow slope on the log N vs log D may result from geometrical or mechanical hardening or because other deformation mechanisms operate in the rock. When duplexes form in rocks, both processes are likely to affect faults within a limited range of lengths. Given the ubiquitous occurrence of duplexes, faceted or stepped log N vs log D plots might be the rule for natural deformations. It is likely that investigators will have already recognized these effects, because one must know the fault intimately to construct a log N vs log D plot. The stepped nature of this plot may, however, provide support for inferences gathered in more typical ways.

Gathering data from different regions within a orogenic belt or from different deformed terranes could mask the effects described here, for anisotropies usually occur at different scales in different locations within a deforming rock mass. While plots constructed using data from different portions of a deformed region may suggest general characteristics of faults in crustal deformation, investigators should recognize that information is lost in combining data from markedly different regimes. Moreover, even if faults from different portions of a deformed region define a characteristic size–frequency relationship, the deformation may not have been self-similar because different faults in that population may have exhibited different characteristics during deformation. Inferences on total strain magnitudes drawn from log N vs log D plots should, therefore, be used cautiously.

Acknowledgements—The Penrose Conference presentations by Randy Marrett and Chris Scholz helped to inspire this contribution. Critical readings by Trent Cladouhos, Mark Brandon and an anonymous referee helped me to sharpen this contribution considerably.

Wendy Kozol helped me with my writing and provided support in innumerable other ways. I thank them all.

REFERENCES

Armstrong, P. A. & Bartley, J. M. 1993. Displacement and deformation associated with a lateral thrust termination, southern Golden Gate Range, southern Nevada, U.S.A. *J. Struct. Geol.* **15**, 721–736.

Aviles, C. A., Scholz, C. H. & Boatwright, J. 1987. Fractal analysis applied to characteristic segments of the San Andreas fault. *J. geophys. Res.* **92**, 331–344.

Boyer, S. E. 1992. Geometric evidence for synchronous thrusting in the southern Alberta and northwest Montana thrust belts. In: *Thrust Tectonics* (edited by McClay, K. R.). Chapman & Hall, London, 377–390.

Boyer, S. E. & Elliott, D. 1982. Thrust systems. *Bull. Am. Ass. Petrol. Geol.* **66**, 1196–1230.

Bruhn, R. L. 1992. Structural and fluid-chemical properties of fault zones. *Geol. Soc. Am. Abs. w. Progr.* **24**, A111.

Childs, C., Walsh, J. J. & Watterson, J. 1990. A method for estimation of the density of fault displacements below the limits of seismic resolution in reservoir formation. In: *North Sea Oil and Gas Reservoirs II* (edited by The Norwegian Institute of Technology). Graham & Trotman, London, 309–318.

Cowie, P. A. & Scholz, C. H. 1992a. Physical explanation for displacement–length relationship of faults using a post-yield fracture mechanics model. *J. Struct. Geol.* **14**, 1133–1148.

Cowie, P. A. & Scholz, C. H. 1992b. Displacement-length scaling relationship for faults: data synthesis and discussion. *J. Struct. Geol.* **14**, 1149–1156.

Eisenstadt, G. & De Paor, D. G. 1987. Alternative model of thrust-fault propagation. *Geology* **15**, 630–633.

Ekstrom, G. & England, P. 1989. Seismic strain rates in regions of distributed continental deformation. *J. geophys. Res.* **94**, 10,231–10,257.

Elliott, D. 1976. The energy balance and deformation mechanics of thrust sheets. *Phil. Trans. R. Soc. Lond.* **A283**, 289–312.

Evans, J. P. 1990. Thickness–displacement relationship of fault zones. *J. Struct. Geol.* **12**, 1061–1065.

Fischer, M. P. & Woodward, N. B. 1992. The geometric evolution of foreland thrust systems. In: *Thrust Tectonics* (edited by McClay, K. R.). Chapman & Hall, London, 181–189.

Gibbs, A. D. 1984. Structural evolution of extensional basin margins. *J. geol. Soc. Lond.* **141**, 609–620.

Grant, N. T., Banks, D. A., McCaig, A. M. & Yardley, B. W. D. 1990. Chemistry, source, and behavior of fluids involved in Alpine thrusting of the Central Pyrenees. *J. geophys. Res.* **95**, 9123–9131.

Hirata, T. 1989. Fractal dimension of fault systems in Japan: Fractal structure in rock fracture geometry at various scales. *Pure & Appl. Geophys.* **131**, 157–170.

Hanks, T. C. 1992. Small earthquakes, tectonic forces. *Science* **256**, 1430–1432.

Harris, L. D. & Milici, R. C. 1977. Characteristics of thin-skinned style of deformation in the southern Appalachians, and potential hydrocarbon traps. *Prof. Pap. U.S. geol. Surv.* **1018**, 1–40.

Holl, J. E. & Anastasio, D. J. 1992. Deformation of a foreland carbonate thrust system, Sawtooth Range, Montana. *Bull. geol. Soc. Am.* **104**, 944–953.

Hubbert, M. K. & Ruby, W. W. 1959. Role of fluid pressure in mechanics of overthrust faulting: I. Mechanics of fluid-filled porous solids and its application to overthrust faulting. *Bull. geol. Soc. Am.* **70**, 115–166.

Hull, J. 1988. Thickness–displacement relationships for deformation zones. *J. Struct. Geol.* **10**, 431–435.

Jackson, J. & McKenzie, D. 1988. The relationship between plate motions and seismic moment tensors, and the rates of deformation in the Mediterranean and Middle East. *Geophys. J. R. astr. Soc.* **93**, 45–73.

Jamison, W. R. 1989. Fault-fracture strain in Wingate Sandstone. *J. Struct. Geol.* **11**, 959–974.

Kakimi, T. 1980. Magnitude-frequency relation for displacement of minor faults and its significance in crustal deformation. *Bull. geol. Surv. Jap.* **31**, 467–487.

Marrett, R. & Allmendinger, R. W. 1990. Kinematic analysis of fault-slip data. *J. Struct. Geol.* **12**, 973–986.

Marrett, R. & Allmendinger, R. W. 1991. Estimates of strain due to brittle faulting: sampling of fault populations. *J. Struct. Geol.* **13**, 735–738.

Marrett, R. & Allmendinger, R. W. 1992. Amount of extension on "small" faults: An example from the Viking graben. *Geology* **20**, 47–50.

Means, W. D. 1984. Shear zones of types I and II and their significance for reconstruction of rock history. *Geol. Soc. Am. Abs. w. Prog.* **16**, 50.

Minor Faults Research Group, 1973. A minor fault system around the Otaki area, Boso Peninsula, Japan. *Earth Sci.* **27**, 180–187.

Mitra, G. 1984. Brittle to ductile transition due to large strains along the White Rock thrust, Wind River Mountains, Wyoming. *J. Struct. Geol.* **6**, 51–61.

Mitra, S. 1986. Duplex structures and imbricate thrust systems: Geometry, structural position, and hydrocarbon potential. *Bull. Am. Ass. Petrol. Geol.* **70**, 1087–1112.

Newman, J. 1993. Characteristics of fault zone deformation: Examples from the southern Appalachians. Unpublished Ph.D. dissertation, University of Rochester, Rochester, New York.

Newman, J. & Mitra, G. 1993. Lateral variations in fault zone thickness as influenced by fluid–rock interactions, Linville Falls fault, North Carolina. *J. Struct. Geol.* **15**, 849–864.

Okubo, P. G. & Aki, K. 1987. Fractal geometry in the San Andreas fault system. *J. geophys. Res.* **92**, 345–355.

Pacheco, J. F., Scholz, C. F. & Sykes, L. R. 1992. Changes in frequency–size relationship from small to large earthquakes. *Nature* **355**, 71–73.

Pettijohn, F. J. 1957. *Sedimentary Rocks* (2nd edn). Harper & Bros. New York.

Platt, J. P. & Leggett, J. K. 1986. Stratal extension in thrust footwalls, Makran accretionary prism: implications for thrust tectonics. *Bull. Am. Ass. Petrol. Geol.* **70**, 191–203.

Roberts, G. 1990. Structural controls on fluid migration in foreland thrust belts. In: *Petroleum and Tectonics in Mobile Belts* (edited by Letouzey, J.). Editions Technip, Paris, 193–210.

Robertson, E. C. 1982. Continuous formation of gouge and breccia during fault displacement. In: *Issues in Rock Mechanics: Proceedings of the 23rd Symposium on Rock Mechanics* (edited by Goodman, R. E. & Heuze, F. E.). American Institute of Mining, Metallurgical and Petroleum Engineers, New York, 397–404.

Robertson, E. C. 1983. Relationship of fault displacement to gouge and breccia thickness. *Miner. Engng* **35**, 1426–1432.

Rye, D. M. & Bradbury, H. J. 1988. Fluid flow in the crust: An example from a Pyreanean thrust ramp. *Am. J. Sci.* **288**, 197–235.

Scholz, C. H. & Cowie, P. A. 1990. Determination of total strain from faulting. *Nature* **346**, 837–839.

Schroeder, M. 1990. *Fractals, Chaos, Power Laws: Minutes From an Infinite Paradise*. W. H. Freeman, New York.

Sibson, R. H. 1989. Earthquake faulting as a structural process. *J. Struct. Geol.* **11**, 1–14.

Swanson, M. T. 1990. Extensional duplexing in the York Cliffs strike-slip fault system, southern coastal Maine. *J. Struct. Geol.* **12**, 499–512.

Tanner, P. W. G. 1992a. Morphology and geometry of duplexes formed during flexural-slip folding. *J. Struct. Geol.* **14**, 1173–1192.

Tanner, P. W. G. 1992b. The duplex model: Implications from a study of flexural-slip duplexes. In: *Thrust Tectonics* (edited by McClay, K. R.). Chapman & Hall, London, 201–208.

Villemin, T. & Sunwoo, C. 1987. Distribution logarithmique self-similaire des rejets et des longeurs de failles: Exemple du Bassin Houllier Lorrain. *C.r.Acad. Sci., Paris* **305**, 1309–1312.

Walsh, J. & Watterson, J. 1988. Analysis of the relationship between displacements and dimensions of faults. *J. Struct. Geol.* **10**, 239–247.

Walsh, J., Watterson, J. & Yielding, G. 1991. The importance of small-scale faulting in regional extension. *Nature* **351**, 391–393.

Watterson, J. 1986. Fault dimensions, displacement, and growth. *Pure & Appl. Geophys.* **24**, 365–373.

Whalley, W. B. & Orford, J. D. 1989. The use of fractals and pseudofractals in the analysis of two-dimensional outlines: Review and further exploration. *Comput. & Geosci.* **15**, 185–197.

Wiltschko, D. V. & Budai, J. M. 1988. A model for fluid motion through layered rock: Evidence from the Idaho–Wyoming thrust belt. *Eos* **69**, 484.

Wojtal, S. 1986. Deformation within foreland thrust sheets by populations of minor faults. *J. Struct. Geol.* **8**, 341–360.

Wojtal, S. 1992. One-dimensional models for plane and non-plane power-law flow in shortening and elongating thrust zones. In: *Thrust Tectonics* (edited by McClay, K. R.). Chapman & Hall, London, 41–53.

Wojtal, S. & Mitra, G. 1986. Strain hardening and strain softening in fault zones from foreland thrusts. *Bull. geol. Soc. Am.* **97**, 674–687.

Wojtal, S. & Mitra, G. 1988. Nature of deformation in fault rocks from Appalachian thrusts. In: *Geometries and Mechanisms of Thrusting with Special Reference to the Appalachians* (edited by Mitra, G. & Wojtal, S.). *Spec. Pap. geol. Soc. Am.* **222**, 17–33.

Woodcock, N. H. & Fischer, M. 1985. Strike-slip duplexes. *J. Struct. Geol.* **8**, 725–735.

Woodward, N. B., Wojtal, S., Paul, J. B. & Zadins, Z. Z. 1988. Partitioning of deformation within several external thrust zones of the Appalachians. *J. geol.* **96**, 351–361.